Observational Study

Medicine®

OPEN

Diagnostic yield, safety, and advantages of ultra-low dose chest CT compared to chest radiography in early stage suspected SARS-CoV-2 pneumonia

A retrospective observational study

Gianluca Argentieri, MD[a], Luca Bellesi, MD[b], Alberto Pagnamenta, MD[c], Gianluca Vanini, MD[d,e], Stefano Presilla, MD[b], Filippo Del Grande, MD[a], Marco Marando, MD[d,*], Pietro Gianella, MD[d,f]

Abstract

To determine the role of ultra-low dose chest computed tomography (uld CT) compared to chest radiographs in patients with laboratory-confirmed early stage SARS-CoV-2 pneumonia.

Chest radiographs and uld CT of 12 consecutive suspected SARS-CoV-2 patients performed up to 48 hours from hospital admission were reviewed by 2 radiologists. Dosimetry and descriptive statistics of both modalities were analyzed.

On uld CT, parenchymal abnormalities compatible with SARS-CoV-2 pneumonia were detected in 10/12 (83%) patients whereas on chest X-ray in, respectively, 8/12 (66%) and 5/12 (41%) patients for reader 1 and 2. The average increment of diagnostic performance of uld CT compared to chest X-ray was 29%. The average effective dose was, respectively, of 0.219 and 0.073 mSv.

Uld CT detects substantially more lung injuries in symptomatic patients with suspected early stage SARS-CoV-2 pneumonia compared to chest radiographs, with a significantly better inter-reader agreement, at the cost of a slightly higher equivalent radiation dose.

Abbreviations: ARDS = acute respiratory distress syndrome, BAL = bronchoalveolar lavage, BMI = body mass index, CRP = C-reactive protein, DAP = dose area product, LDH = lactic acid dehydrogenase, rRT-PCR = real-time reverse transcription-polymerase chain reaction, SARS-CoV-2 = severe acute respiratory syndrome-coronavirus 2, uld CT = ultra-low dose computed tomography, WHO = World Health Organization.

Keywords: chest CT, computed tomography, dose optimization, safety, SARS-CoV-2 ;

1. Introduction

The novel coronavirus-2 (SARS-CoV-2) infection with associated severe acute respiratory syndrome originated in China in December 2019 and reached the Lombardy region of northern Italy 2 months later.[1] Ticino is the Swiss canton neighboring Lombardy in which the first Swiss cases were diagnosed on February 25, 2020.[2] On the March 11, 2020, the World Health Organization (WHO) declared SARS-CoV-2 a pandemic. At the time of the writing of this article infections due to SARS-CoV-2 continue to increase worldwide.[3] The most frequent symptoms of pneumonia caused by SARS-CoV-2 are fever and cough. Approximately 5% of infected patients are admitted to intensive care units.[4] Significant increases in C-reactive protein (CRP) and lactic acid dehydrogenase (LDH) as well as lymphocytopenia are present in most patients with SARS-CoV-2 and are considered negative prognostic indicators.[4,5] Moreover, an increase of these biological parameters seems to correlate with the extension of infiltrates seen on chest computed tomography (CT) scans.[6]

The viral nucleic acid test, real-time reverse transcription-polymerase chain reaction (rRT-PCR) assay, has played a pivotal role in the diagnosis of SARS-CoV-2 and in clinical decision-making regarding hospitalization and isolation of individual patients. However, its imperfect sensitivity, insufficient stability, and relatively long processing time have proven this test to be insufficient for timely characterization in the acute clinical setting

Editor: Anil Jha.

The authors report no conflict of interest, in particular did not receive any funding from NIH, Wellcome Trust, or HHMI.

The datasets generated during and/or analyzed during the present study are not publicly available but are available from the corresponding author on reasonable request.

[a] IIMSI – Radiology Department, Ospedale Regionale di Lugano, [b] IIMSI – Medical Physics, Ospedale San Giovanni, [c] Intensive Care Unit, Ospedale Beata Vergine, [d] Internal Medicine Department, [e] Allergology, Internal Medicine Department, [f] Pneumology, Ospedale Regionale di Lugano, Ente Ospedaliero Cantonale, Switzerland.

[*] Correspondence: Marco Marando, Internal Medicine Department, Ospedale Regionale di Lugano, Via Tesserete 46, 6900 Lugano, Switzerland (e-mail: marco.marando@eoc.ch).

How to cite this article: Argentieri G, Bellesi L, Pagnamenta A, Vanini G, Presilla S, Del Grande F, Marando M, Gianella P. Diagnostic yield, safety, and advantages of ultra-low dose chest CT compared to chest radiography in early stage suspected SARS-CoV-2 pneumonia: a retrospective observational study. Medicine 2021;100:21(e26034).

Received: 29 March 2021 / Received in final form: 30 April 2021 / Accepted: 3 May 2021

http://dx.doi.org/10.1097/MD.0000000000026034

and for the progression of the pandemic.[7] The front-line radiological examination performed in these patients is usually a conventional chest radiograph, yet this modality has proven to be of limited value due to frequent false-negative results.[8] By comparison, chest CT has proven to be more sensitive, with well-documented features in patients with SARS-CoV-2 pneumonia[9], such as sub-pleural (peripheral), multifocal, and bilateral ground-glass opacities being commonly observed in more than half of patients.[6,10,11] In the second phase of the disease, characteristic CT signs of lung damage such as crazy-paving patterns or consolidations may appear.[12] Several studies have demonstrated the evolution of chest CT findings of SARS-CoV-2 pneumonia by classifying its radiological characteristics at different stages of infection.[13–15] Specifically, in a retrospective study, chest CTs of 121 symptomatic patients infected with SARS-CoV-2 were reviewed and during the first 2 days of SARS-CoV-2 infection, chest CT scans showed no infiltrates in half of the patients. Subsequently (between days 6 and 12), infiltrates appear in >90% of cases.[15] Chest CT demonstrates a low false-negative rate in the diagnosis of SARS-CoV-2 pneumonia[16] and has been used to support the effectiveness of anti-inflammatory or non-specific antiviral therapies in a later phase of the disease.[17–19] Therefore, CT is a useful tool for diagnosis, management, and therapeutic follow-up of SARS-CoV-2 pulmonary infections. Moreover, CT scan proved valuable to evaluate the mid- and long-term consequences of SARS-CoV-2 pneumonia. [20–23] Nevertheless, medical radiation exposure remains an ever-important issue due to the broad range of the patient population affected by the pandemic, which includes all ages, as well as young individuals.[24] New technologies and protocols such as ultra-low dose CT (uld CT) identify individual cases not seen on conventional radiography and can be implemented as a means of large-scale public health surveillance with reduced radiation exposures.[25–27] Therefore, in epicenters of the pandemic, uld CT could be used as a screening tool or as an adjunct to rRT-PCR to exclude occult infection, especially prior to surgery or intensive immunosuppressive therapies. The purpose of this study was to evaluate the diagnostic yield, utility, and advantages of chest uld CT compared to that of conventional chest radiographs in patients suspected of early stage pneumonia with laboratory-confirmed SARS-CoV-2.

2. Materials and methods

We reviewed 12 consecutive cases of patients with suspected SARS-CoV-2 pneumonia admitted to our Regional Hospital (Ospedale Regionale di Lugano, Ticino, Switzerland) from March 2, 2020 through March 12, 2020. A suspected SARS-CoV-2 case was defined as a patient presenting fever (≥38°C) or respiratory symptoms (cough, dyspnea). Clinical samples for SARS-CoV-2 diagnostic testing were obtained in accordance with WHO guidelines. Nasopharyngeal and oropharyngeal swab specimens were collected with synthetic fiber swabs and the swabs were inserted into the same sterile tube containing 2 to 3 mL of viral transport medium. Influenza, Pneumococcus, and Legionella tests excluded other possible intercurrent infections. In 1 case virus identification was carried out with bronchoalveolar lavage (BAL) and specimens were extracted and subjected to next-generation sequencing. All patients (100%, 12) resulted in SARS-CoV-2 positive in rRT-PCR tests, which we considered the reference standard for the purposes of our study. The study was approved by the ethics committee of Southern Switzerland and it was performed in accordance with relevant guidelines and regulations.

2.1. Chest X-ray and CT protocol

To identify any signs of pneumonia at admission in the emergency room, all patients suspected of SARS-CoV-2 underwent a baseline digital anteroposterior chest radiography at full inspiration using a mobile chest radiograph device (Philips Mobile Diagnost wDR, Philips Medical System SA). We performed chest uld CT in patients with signs of respiratory failure ($FIO_2/PaO_2 < 300$ mmHg), with clinical SARS-CoV-2 compatible symptoms or with suspicious SARS-CoV-2 parenchymal changes at chest X-ray. Chest uld CT images were obtained at 22.5 ± 14.1 hours (range, 3–48 hours) from chest X-ray acquisition using 2 multi-detector scanners: Siemens Somatom Definition Flash and Siemens Somatom Definition Edge (Siemens, Erlangen, Germany). Scan parameters were optimized for a patient with a normal BMI between 18.5 and 24.9 as follows: tube voltage 80 kVp; fix tube current of 20 mAs without automatic exposure control; slice thickness 2.0 mm; reconstruction interval 2 mm; with a sharp reconstruction kernel. CT images were acquired with the patient in the supine position at full inspiration, without intravenous contrast medium.

2.2. Image analyses

Two radiologists with different specialty skills: thoracic, reader 1 (R1) and general, reader 2 (R2), with respectively 10 and 17 years of experience (GA and FDG), reviewed both chest radiographs and CT images on 2 different days to reduce the recall bias. On the first day, the readers reviewed the chest radiographs and on the second day the CT scans, both series randomly presented. The CT images were evaluated with both lung (width, 1500 HU; level, −600 HU) and mediastinal (width, 400 HU; level, 40 HU) window settings. Images were reviewed on a professional picture archiving and communication system (PACS) PC workstation (Philips Intellispace PACS). For the purpose of our study, a peripheral location was defined as the outer third of the lung parenchyma. The readers assessed both chest radiographs and uld CT only for the presence of parenchymal abnormalities compatible with SARS-CoV-2 infections. The number of lobes involved (from 0 to 5 lobes), the location (central, peripheral, or both), and opacity density (ground-glass, consolidation, or both) based on the Fleischner Society glossary of terms for thoracic imaging were annotated.[28] Mediastinal and osseous structures were not evaluated.

2.3. Dose analyses

CT effective dose and equivalent organ dose calculation were obtained with Radimetrics (Bayer Medical Care Inc., Indianola, PA, USA), a web-based software platform, using an available Monte Carlo interactive dosimetry tool essentially superimposing real CT images with virtual Christy phantoms available inside the software. The software automatically matched the phantom and the patient scanogram and calculated the organ-specific radiation doses as well as the global radiation parameter, expressed in mSv, according to the tissue weighting factors reported in International Commission on Radiological Protection (ICRP) 103 and in ICRP 60.[29] Dose area product (DAP) and patient data related to each radiographic exam were transferred into Radimetrics. After data

collection, the PC-based Monte Carlo program for X-ray simulation, PCXMC (STUK, Helsinki, Finland), was used to calculate the effective dose, organ doses, and assessment of exposure for radiographic exams.[30]

2.4. Statistical analyses

For descriptive statistics, categorical variables were expressed as absolute numbers with percentages, normally distributed quantitative variables as mean ± standard deviation (SD) and non-normally distributed variables as median with an inter-quartile range (IQR). To assess the agreement between the 2 radiologists concerning the different radiological categorical variables, kappa statistics were presented as follows: 0 very poor; 0.01 to 0.20 poor; 0.21 to 0.40 discreet; 0.41 to 0.60 moderate; 0.61 to 0.80 good; and 0.81 to 1.00 excellent.[31] Stata version 15 (StataCorp. LP, College Station, TX, USA) was used for all statistical analyses.

3. Results

3.1. Clinical findings

A total of 12 laboratory-proven SARS-CoV-2 patients (mean age, 57.8 ± 13.6 years, 58% male) were included. Three patients (25%) fulfilled the criteria of mild (200 mm Hg < $PaO_2/FIO_2 \leq$ 300 mm Hg) Acute Respiratory Distress Syndrome (ARDS) and 1 (8%) the criteria of moderate (100 mm Hg < $PaO_2/FIO_2 \leq 200$ mm Hg) ARDS. We observed CRP elevations in 83% of patients (mean CRP, 78 ± 76 mg/L). LDH could be assessed in 10 out of 12 patients and in 9 out of 10 (90%) we recorded elevated values (mean LDH, 475 ± 220 mg/L) (Table 1.). Two out of 12 patients (16%) had positive urinary antigens for Legionella and pneumococcus and 2 out of 12 patients (16%) had positive swab results for Influenza A, B, and Respiratory Syncytial Virus.

3.2. Inter-reader-, chest radiographic- and CT-findings

R1 reported the absence of radiographic abnormalities (ground glass, consolidation, or both) in 4 (33%) patients and R2 reported the absence of these findings in 7 patients (58%). The inter-reader agreement for bilateral distribution was moderate (kappa value = 0.5). On chest radiographs, the distribution of abnormalities was described in the sub-pleural regions in 6 patients (50%) by R1 and in 1 patient (8%) by R2 (kappa value = 0.5). A central location and combined central and peripheral locations were observed respectively in 4 patients (33%) by R1 and in 0 patients (0%) by R2 (kappa value = 0.62), and in 2 patients (16%) by R1 and in 4 patients (33%) by R2 (kappa value = 0.57) (Table 2). By contrast, on chest uld CT both readers excluded parenchymal abnormalities (ground-glass, consolidation, or both) in 16% of the cases. At CT the inter-observer agreement for bilateral distribution was perfect (kappa value = 1). The distributions of these abnormalities on uld CT were described in subpleural regions in 9 patients (75%) by R1 and in 10 patients (83%) by R2 (kappa value = 0.75); in a predominantly central location in 9 patients (75%) by R1 and in 8 patients (66%) by R2 (kappa value = 0.8); and in both central and peripheral locations in 8 patients (66%) by both R1 and R2 (kappa value = 1) (Table 2). At uld CT abnormalities in 10/12 (83%) SARS-CoV-2 patients were detected by both readers with

Table 1

Clinical characteristics of the patients.

Patient	1	2	3	4	5	6	7	8	9	10	11	12
Sex	F	M	F	M	F	M	F	M	F	M	M	M
Age	47.6	58.5	57.0	62.1	45.1	46.9	81.1	70.9	50.6	83.3	44.1	50.1
CRP, mg/L (<5)	113	2	74	18	2	271	91	29	14	98	133	86
LDH, U/L (140–280)	479	506	534	456	270	578	466	–	–	514	906	383
FIO_2/PaO_2, mmHg (>400)	236	325	321	336	432	196	204	400	321	275	368	375

CRP = C-reactive protein, LDH = lactate dehydrogenase.

Table 2

Radiological findings for reader 1 and 2 for chest radiographs and ultra-low dose CT.

	RX		CT	
	R1	R2	R1	R2
No. of lobes affected	100% (12/12)	100% (12/12)	100% (12/12)	100% (12/12)
0	33% (4/12)	58% (7/12)	16% (2/12)	16% (2/12)
1	8% (1/12)	8% (1/12)	8% (1/12)	8% (1/12)
2	8% (1/12)	8% (1/12)	16% (2/12)	16% (2/12)
3	41% (5/12)	8% (1/12)	25% (3/12)	8% (1/12)
4	0% (0/12)	8% (1/12)	0% (0/12)	0% (0/12)
5	8% (1/12)	8% (1/12)	33% (4/12)	50% (6/12)
Ground-glass opacities	58% (7/12)	8% (1/12)	75% (9/12)	33% (4/12)
Consolidation	41% (5/12)	33% (4/12)	16% (2/12)	8% (1/12)
Ground-glass opacities and consolidation	33% (4/12)	0% (0/12)	8% (1/12)	41% (5/12)
Bilateral disease	50% (6/12)	25% (3/12)	75% (9/12)	75% (9/12)
Peripheral distribution	50% (6/12)	8% (1/12)	75% (9/12)	83% (10/12)
Central distribution	33% (4/12)	0% (0/12)	75% (9/12)	66% (8/12)
Central and peripheral distribution	16% (2/12)	33% (4/12)	66% (8/12)	66% (8/12)

CT = computed tomography.

a sensitivity of 83%. Using uld CT as a reference, pulmonary abnormalities compatible with SARS-CoV-2 pneumonia were detected when using chest X-ray in 8/12 (66%) cases by R1 and in 5/12 (41%) cases by R2. These values corresponded with the chest X-ray sensitivity for each reader. The average sensitivity for this method was therefore 54%. All lobes were reported to be affected on chest radiographs, respectively, 0/12 (0%) by R1 and in 1/12 (8%) by R2, which differed at uld CT with 4/12 (33%) patients by R1 and 6/12 (50%) patients by R2. The increment of diagnostic performance for R1 with uld CT was about 16% higher than chest X-ray while for R2 was 42%, with an average value of 29% for both readers. Given the absence of asymptomatic or negative SARS-CoV-2 patients in our population in our study, specificity, VPP, and VPN were not calculated. For the same reason, accuracy for chest radiography and uld CT corresponded with the sensitivities of both diagnostic modalities.

3.3. Dosimetry results

For chest radiography, the average effective dose was 0.073 mSv with an average lung equivalent dose of 0.143 mSv and an average DAP equal to 194 mGy cm^2 (Tables 3 and 4). For uld CT average effective dose was 0.219 mSv while the average lung equivalent dose was 0.498 mSv with an average CT dose index (CTDI) value equal to 0.433 mGy and average dose-length product (DLP) value of 14.3 mGy cm (Tables 5 and 6). At our institution dosimetry values for a standard low-dose chest CT are as follows: CTDI: 3.3 ± 1.102 mGy; DLP: 121.1 ± 49.23 mGy cm;

Table 3

Exam data and dose estimations for radiographic exams with PCXMC.

Radimetrics data					PCXMC	
No. patient	Projection	kV	Proiection	DAP (mGy cm^2)	Dose to lungs (mSv)	Effective dose ICRP 103 (mSv)
1	Supine	100	AP	104.7	0.073	0.037
2	Standing	100	AP	162.0	0.135	0.067
3	Supine	100	AP	178.8	0.140	0.075
4	Supine	102	AP	226.2	0.173	0.089
5	Sitting	100	AP	198.0	0.153	0.079
6	Supine	100	AP	120.5	0.094	0.048
7	Sitting	100	AP	108.6	0.087	0.045
8	Standing	125	AP+LAT	340.4	0.146	0.069
9	Standing	100	AP	361.3	0.284	0.149
10	Supine	117	AP	165.7	0.140	0.071
11	Supine	100	AP	157.0	0.121	0.062
12	Supine	100	AP	209.5	0.164	0.088

DAP = dose area product.

Table 4

Statistical data analysis for radiographic exams.

Radiography	DAP (mGy cm^2)	Dose to lungs (mSv)	Effective dose ICRP 103 (mSv)
MEDIA	194.4	0.143	0.073
MEDIAN	172.3	0.140	0.070
75 percentile	213.7	0.156	0.081
St.Dev.	82.5	0.054	0.029

DAP = dose area product.

Table 5

Exam data and dose estimations for CT exams with Radimetrics.

Radimetrics					
No. patient	Date of CT	CTDI (mGy)	DLP (mGy cm^2)	Effective dose ICRP 103 (mSv)	Equivalent dose to lung (mSv)
1	43897	0.4	15	0.171	0.427
2	43893	0.4	12.8	0.289	0.615
3	43897	0.4	12.9	0.263	0.545
4	43896	0.5	17	0.279	0.657
5	43896	0.5	16.3	0.159	0.391
6	43903	0.4	15	0.188	0.455
7	43901	0.5	17.3	0.166	0.398
8	43899	0.4	9.9	0.22	0.499
9	43902	0.5	14.8	0.288	0.571
10	43897	0.4	13.9	0.207	0.528
11	43899	0.4	13.3	0.155	0.404
12	43902	0.4	13.1	0.239	0.485

CT = computed tomography.

Table 6

Statistical data analysis for CT exams.

CT	CTDI (mGy)	DLP (mGy cm^2)	Effective dose ICRP 103 (mSv)	Equivalent dose to lung (mSv)
Media	0.433	14.275	0.219	0.498
Median	0.400	14.350	0.214	0.492
75 percentile	0.500	15.325	0.267	0.552
St.Dev.	0.049	2.082	0.052	0.088

CT = computed tomography.

effective dose: 2.31 ± 0.81 mSv. Data were extracted with Radimetrics.

4. Discussion

In our study, ultra-low dose CT proved to be a non-invasive imaging modality with slightly higher radiation dose, but with substantially higher accuracy and much higher inter-reader agreement compared to chest radiography. The average effective dose of chest radiography taken in just 1 projection was 0.073 mSv at our institution. Typical effective dose reported for chest radiography should have values lower than 0.07 mSv depending on age and specific conditions.[26,32] According to our results, the average effective dose recorded for a chest uld CT was 0.219 mSv, meaning that the average effective dose of a chest uld CT was about 3 times higher than that of a chest radiograph. In the current literature, chest uld CT is usually associated with a radiation dose varying from 0.14 to 0.5 mSv.[25,26] For this dose range no standardized reference values have been published as of yet.

In our series, up to 58% of patients with SARS-CoV-2 suspected pneumonia had a negative chest X-ray. This data underpins the limited diagnostic value of chest X-ray, due to the prevalence of false-negative results.[8] In our study, uld CT resulted positive for the presence of suspicious pulmonary ground-glass infiltrates or consolidations in 83% of the cases. A larger Chinese study by Ai et al demonstrated 88% positive cases by utilizing low-dose chest CT.[33] Our study demonstrated that at early ($\leq$48 h) chest uld CT ground-glass infiltrates, with or without consolidation, presented predominantly in combined locations peripheral and central (kappa value = 1), with chiefly bilateral involvement (kappa value = 1). These results are similar to those studies of viral pneumonia described in the literature which utilized standard chest CT.[10,11,13] On chest radiographs, most of the pulmonary alterations had ambiguous localizations. The concordance of infiltrate distribution among each lobe for both readers was poor (kappa value = 0.33). Ground-glass infiltrates were difficult to evaluate (kappa value = 0.13), while the concordance for consolidation was higher (kappa value = 0.47). This is probably due to readers' subjective interpretations of density and radiographic transparency. At uld CT, ground-glass infiltrates proved easier to evaluate and agreement to that of chest radiographs was superior (kappa value = 0.55) although, probably due to the heterogeneity of the involvement of the lung parenchyma, agreement on infiltrate distribution among each lobe, as well as agreement on the evaluation of regions of pulmonary consolidation were poor (kappa value = 0.33). In accordance with the findings of Yoon et al, our experience confirms that chest X-ray still underestimates the diagnosis of SARS-CoV-2 pneumonia even when compared to an ultra-low dose CT protocol.[8] We discovered that in cases where all lobes were involved on uld CT images (33–50% of cases), only 0–8% of chest radiographs appeared abnormal. The performance of both readers improved by approximately 29% using uld CT,

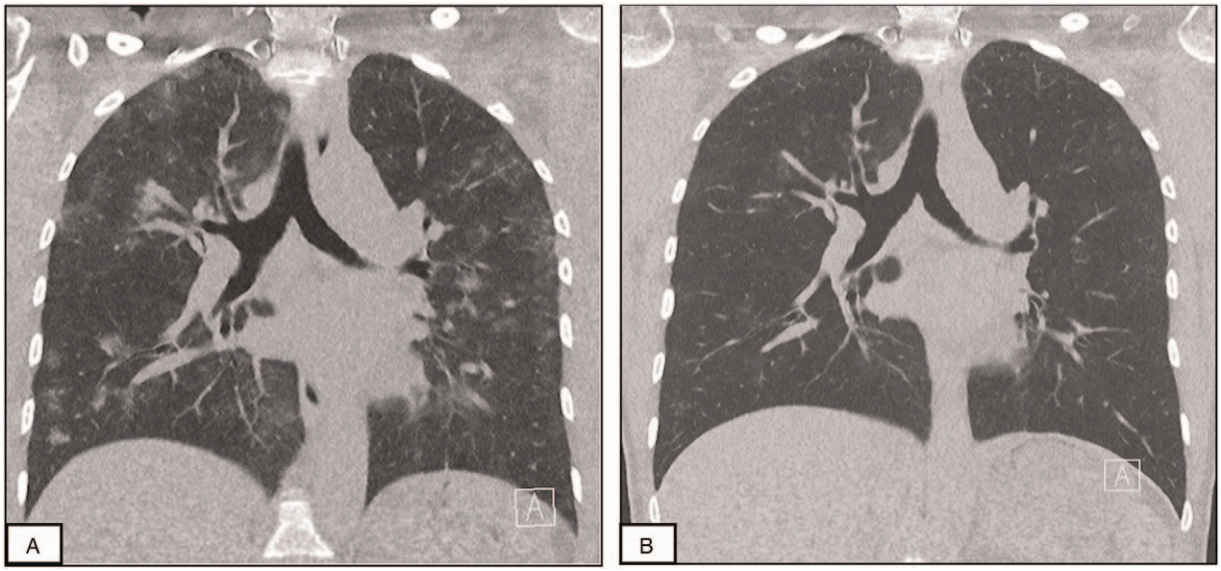

Figure 1. Patient 1: evolution with progressive healing of lung infiltrates on chest ultra-low dose CT. Progressive healing from day 1 (A) to day 15 (B) of typical bilateral infiltrates with subpleural distribution.

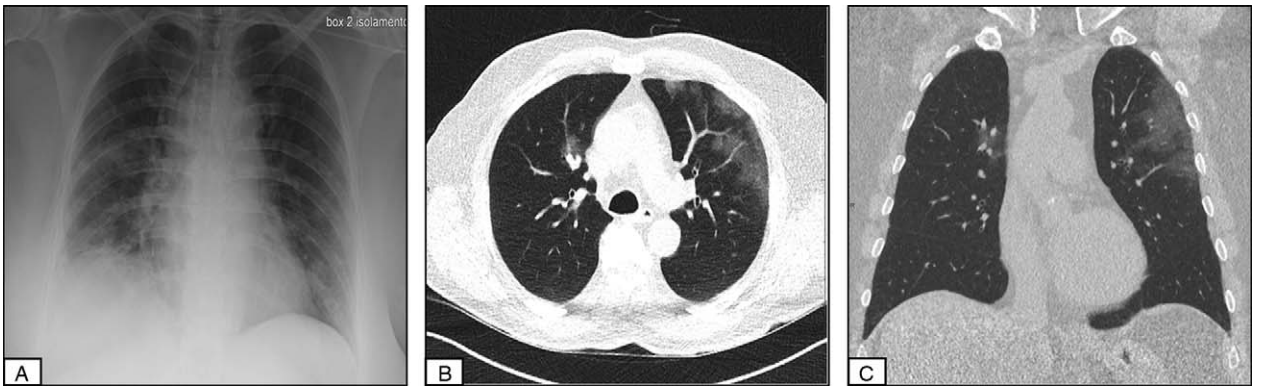

Figure 2. Patient 3: lung infiltrates on chest X-ray and chest ultra-low dose CT. Chest X-ray showed ill-defined infiltrates on the right mid and basal fields (A). Ultra-low dose CT showed diffuse bilateral infiltrates (B and C).

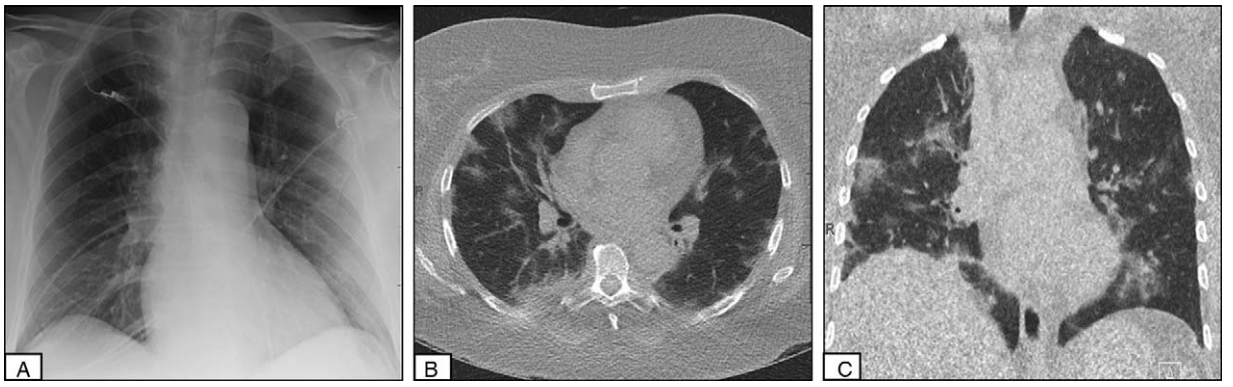

Figure 3. Patient 8: suboptimal, apparently unremarkable chest radiograph (A). Conversely, ultra-low dose CT showed patchy bilateral areas of ground-glass opacifications (B and C).

when compared to that demonstrated with chest radiography. This improvement proved even higher (42%) for the general radiologist, suggesting that this modality could assist radiologists not sub-specialized in thoracic radiology, particularly during this critical pandemic period when there is an abundance of thoracic exams. Therapy management was also assessed in our series using uld CT. In 1 case, therapy involving 3 days of treatment with aspecific anti-inflammatory and antiviral therapy followed by 10 days of remdesivir demonstrated progressive healing documented by uld CT follow-up examinations on day 9 and 15 (Fig. 1A and B). Other studies have already used standard chest CT to document therapeutic follow-up in similar cases treated with non-specific anti-viral antibodies[15], but not with a chest uld CT protocol. High suspicion for SARS-CoV-2 infection can be triggered by a typical radiological chest finding, even when an rRT-PCR test results negative. In a second case, chest radiographs showed ill-defined bilateral abnormalities (Fig. 2A) with SARS-CoV-2 nasopharyngeal and oral swabs negative on admission. Chest uld CT showed instead typical diffuse ground-glass infiltrates, highly suggestive of viral pneumonia (Fig. 2B and C). The swab test was repeated and resulted again negative, whereupon a third test obtained by BAL finally confirmed the diagnosis of SARS-CoV-2 pneumonia. In a third and last case, a chest X-ray performed in the sitting position initially did not show clear infiltrates (Fig. 3A) despite the clinical suspicion of SARS-CoV-2 infection, which was later confirmed by laboratory results. Chest uld CT revealed the presence of typical subpleural ground-glass opacities in both upper lobes, highly consistent with SARS-CoV-2 viral pneumonia (Fig. 3B and C). The last 2 cases demonstrate the critical diagnostic value of chest uld CT.

This study has some limitations. First, the number of included patients was small, because of the very early phase of the pandemic in our region at the time of data collection (180 new registered cases up to 12th of March).[34] Second, the study was retrospective and despite the median for the delay between chest X-ray and chest uld CT examinations being 22.5 hours, the range was wide (3–48 hours). This wide range could potentially interfere with the correlation of findings between these 2 modalities but suggests a time that could have been saved if uld CT was the first and only modality used. Third, the PCXMC phantoms have 2 potential limitations for accurate dosimetry: over-simplified stylized phantoms and anatomical structures not completely comparable to voxel or hybrid phantoms potentially lead to an unrealistic, over-simplified adjustment of body size.

5. Conclusions

In summary, our results suggest that chest uld CT detects a substantially larger burden of inflammatory changes, with a much higher inter-reader agreement, in patients with early stage

suspected SARS-CoV-2 pneumonia when compared to conventional chest radiography, at the cost of a slightly higher equivalent radiation dose. In patients with high clinical suspicion and negative rRT-PCR results, implementing the ultra-low dose chest CT protocol can improve diagnostic performance during the early phase of this disease.

Acknowledgments

We are grateful to all the colleagues, the nurses, and the staff of the Ospedale Regionale in Lugano for their relentless support and their precious work in facing this dreadful pandemic.

Author contributions

Conceptualization: Gianluca Argentieri, Luca Bellesi, Stefano Presilla, Pietro Gianella.
Data curation: Gianluca Argentieri, Luca Bellesi, Pietro Gianella.
Formal analysis: Alberto Pagnamenta, Stefano Presilla.
Investigation: Stefano Presilla.
Methodology: Gianluca Argentieri, Alberto Pagnamenta.
Project administration: Gianluca Argentieri, Pietro Gianella.
Supervision: Luca Bellesi, Alberto Pagnamenta, Stefano Presilla, Filippo Del Grande, Pietro Gianella.
Validation: Pietro Gianella.
Visualization: Gianluca Vanini, Stefano Presilla, Filippo Del Grande, Marco Marando, Pietro Gianella.
Writing – original draft: Gianluca Argentieri.
Writing – review & editing: Alberto Pagnamenta, Gianluca Vanini, Stefano Presilla, Filippo Del Grande, Marco Marando, Pietro Gianella.

References

[1] Tian S, Hu N, Lou J, et al. Characteristics of COVID-19 infection in Beijing. J Infect 2020;80:401–6.
[2] COVID19 (DSS) – Repubblica e Cantone Ticino. Available at: https://www4.ti.ch/dss/dsp/covid19/home/#c542050. Accessed April 27, 2021.
[3] WHO COVID Dashboard. Available at: https://covid19.who.int/?gclid=Cj0KCQiAoab_BRCxARIsANMx4S73rkrbCXYza2HYxwfWBTCrmC5i4Hwe–K-Z92hRqH2hKpTaJOZfxYaAplrEALw_wcB. Accessed April 27, 2021.
[4] Guan WJ, Ni ZY, Hu Y, et al. Clinical characteristics of coronavirus disease 2019 in China. N Engl J Med 2020;30:1708–20.
[5] Huang C, Wang Y, Li X, et al. Clinical features of patients infected with 2019 novel coronavirus in Wuhan, China. Lancet 2020;395:497–506.
[6] Xiong Y, Sun D, Liu Y, et al. Clinical and high-resolution CT features of the COVID-19 infection: comparison of the initial and follow-up changes. Invest Radiol 2020;55:332–9.
[7] Yang Y, Yang M, Yuan J, et al. Laboratory diagnosis and monitoring the viral shedding of SARS-CoV-2 infection. Innovation 2020;1–3.
[8] Yoon SH, Lee KH, Kim JY, et al. Chest radiographic and CT findings of the 2019 novel coronavirus disease (COVID-19): analysis of nine patients treated in Korea. Korean J Radiol 2020;21:494–500.
[9] Kanne JP, Little BP, Chung JH, Elicker BM, Ketai LH. Essentials for radiologists on COVID-19: an update-radiology scientific expert panel. Radiology 2020;27:200527.
[10] Zhou S, Wang Y, Zhu T, Xia L. CT features of coronavirus disease 2019 (COVID-19) pneumonia in 62 patients in Wuhan, China. Radiology 2020;4:200230.
[11] Kanne JP. Chest CT findings in 2019 novel coronavirus (2019-nCoV) infections from Wuhan, China: key points for the radiologist. Radiology 2020;295:16–7.
[12] Chung M, Bernheim A, Mei X, et al. CT imaging features of 2019 novel coronavirus (2019-nCoV). Radiology 2020;295:202–7.
[13] Shi H, Han X, Jiang N, et al. Radiological findings from 81 patients with COVID-19 pneumonia in Wuhan, China: a descriptive study. Lancet Infect Dis 2020;20:425–34.
[14] Pan Y, Guan H, Zhou S, et al. Initial CT findings and temporal changes in patients with the novel coronavirus pneumonia (2019-nCoV): a study of 63 patients in Wuhan, China. Eur Radiol 2020;30:3306–9.
[15] Bernheim A, Mei X, Huang M, et al. Chest CT findings in coronavirus disease-19 (COVID-19): relationship to duration of infection. Radiology 2020;295:200463.
[16] Li Y, Xia L. Coronavirus disease 2019 (COVID-19): role of chest CT in diagnosis and management. AJR Am J Roentgenol 2020; 214:1280–6.
[17] Duan YN, Qin J. Pre- and posttreatment chest CT findings: 2019 novel coronavirus (2019-nCoV) pneumonia. Radiology 2020;295:21.
[18] Lei J, Li J, Li X, Qi X. CT imaging of the 2019 novel coronavirus (2019-nCoV) pneumonia. Radiology 2020;295:18.
[19] Wei J, Xu H, Xiong J, et al. 2019 novel coronavirus (COVID-19) pneumonia: serial computed tomography findings. Korean J Radiol 2020;21:501–4.
[20] Gianella P, Rigamonti E, Marando M, et al. Clinical, radiological and functional outcomes in patients with SARS-CoV-2 pneumonia: a prospective observational study. BMC Pulm Med 2021;21:136.
[21] Huang C, Huang L, Wang Y, et al. 6-month consequences of COVID-19 in patients discharged from hospital: a cohort study. Lancet 2021; 397:220–32.
[22] Guler SA, Ebner L, Beigelman C, et al. Pulmonary function and radiological features four months after COVID-19: first results from the national prospective observational Swiss COVID-19 lung study. Eur Respir J 2021; in press.
[23] González J, Benítez ID, Carmona P, et al. Pulmonary function and radiological features in survivors of critical COVID-19: a 3-month prospective cohort. Chest 2021.
[24] Kang Z, Li X, Zhou S. Recommendation of low-dose CT in the detection and management of COVID-2019. Eur Radiol 2020;1–2.
[25] Kim Y, Kim YK, Lee BE, et al. Ultra-low-dose CT of the thorax using iterative reconstruction: evaluation of image quality and radiation dose reduction. AJR Am J Roentgenol 2015;204:1197–202.
[26] Vilar-Palop J, Vilar J, Hernández-Aguado I, González-Álvarez I, Lumbreras B. Updated effective doses in radiology. J Radiol Prot 2016;6:975–90.
[27] Kroft LJM, van der Velden L, Girón IH, Roelofs JJH, de Roos A, Geleijns J. Added value of ultra-low-dose computed tomography, dose equivalent to chest X-ray radiography, for diagnosing chest pathology. J Thorac Imaging 2019;4:179–86.
[28] Rubin GD, Ryerson CJ, Haramati LB, et al. The role of chest imaging in patient management during the COVID-19 pandemic: a multinational consensus statement from the Fleischner Society. Chest 2020;158: 106–16.
[29] The 2007 recommendations for the International Commission on Radiological Protection. ICRP publication 103. Ann ICRP 2007;37:1–332.
[30] Tapiovaara M, Siiskonen T. PCXMC—a Monte Carlo Program for calculating patient doses in medical X-ray examinations. STUK-A231 2nd ed.Helsinki: STUK; 2008. Available at: https://www.stuk.fi/documents/12547/474783/stuk-a231.pdf/c950e99c-3537-4344-bf76-07a54e5f1afa?t=1439557836831. Accessed April 27, 2021
[31] Landis JR, Koch GG. The measurement of observer agreement for categorical data. Biometrics 1977;33:159–74.
[32] Accuracy of ultra-low-dose CT (ULDCT) of the chest compared to plain film in an unfiltered emergency patient cohort. Available at: https://clinicaltrials.gov/ct2/show/NCT03922516. Accessed April 27, 2021.
[33] Ai T, Yang Z, Hou H, et al. Correlation of chest CT and RT-PCR testing in coronavirus disease 2019 (COVID-19) in China: a report of 1014 cases. Radiology 2020;26:200642.
[34] Nuovo coronavirus: Situazione in Svizzera (2020). Available at: https://www.bag.admin.ch/bag/it/home/krankheiten/ausbrueche-epidemien-pandemien/aktuelle-ausbrueche-epidemien/novel-cov/situation-schweiz-und-international.html#-1674360640. Accessed April 27, 2021.